FATIGUE BEHAVIOR OF RC BEAMS STRENGTHENED WITH GFRP SHEETS

By Christos G. Papakonstantinou,[1] Michael F. Petrou,[2] and Kent A. Harries[3]

ABSTRACT: The objective of the presented study is to examine the effects of glass fiber reinforced polymer (GFRP) composite rehabilitation systems on the fatigue performance of reinforced concrete beams. Experiments were conducted on beams with and without GFRP composite sheets on their tensile surfaces. The specimens were 152 × 152 × 1,321 mm reinforced concrete beams with enough transverse reinforcement to avoid shear failure. The results of this study indicate that the fatigue life of reinforced concrete beams with the given geometry, subjected to the same cycling load, can be significantly extended through the use of externally bonded GFRP composite sheets. An interesting finding is that, although the fiber strengthening system increases the fatigue life of the beams, the failure mechanism, fatigue of the steel reinforcement, remains the same in both strengthened and nonstrengthened beams. Thus, it is possible to predict the fatigue life of a cyclically loaded beam using existing fatigue models.

INTRODUCTION

Fiber reinforced polymer (FRP) composite materials have been successfully used in new construction and for the repair and rehabilitation of existing structures. It is the latter use where FRP materials hold the greatest promise. Strengthening or stiffening of reinforced concrete and prestressed concrete structures may be required as a result of an increase in load requirements, a change in use, natural or man-made degradation of the structure, or design or construction defects. Repair with externally bonded FRP reinforcement is attractive to owners, engineers, and contractors because of the ease and speed of installation, the structural efficiency of the repair, the corrosion resistance of the materials, and the minimal effect that these materials have on structural dimensions aesthetics, and versatility.

Although many tests have been conducted investigating strengthening reinforced concrete members with FRP composite materials, there are still many aspects of their use that remain to be investigated. The fatigue behavior of reinforced concrete beams strengthened with FRP composite sheets, for instance, which is described in this paper, provides valuable information regarding the long-term performance of the FRP strengthening systems.

BACKGROUND

In recent years, considerable interest has developed in the fatigue behavior of reinforced concrete members. There are several reasons for this interest. The widespread adoption of ultimate strength design procedures and the use of higher strength and more durable materials require that structural concrete members perform satisfactorily under high stress levels for a longer period of time. There is also a new recognition of the effects of repeated loading on a member, even if repeated loading does not cause a fatigue failure. Repeated loading may lead to internal cracking of a member that alters its stiffness and load-carrying characteristics (ACI Committee 215 1992).

There has been significant research conducted on the fatigue of reinforcing steel (Helgason and Hanson 1974; Corely et al. 1978; Tilly 1979; Moss 1982), plain concrete (Shah and Chandra 1970; Hordijk and Reinhardt 1992) and the bond between the steel and concrete (Rehm and Eligehausen 1979; Balazs 1991). Verna and Stelson (1962) did some limited work on reinforced concrete beams in the 1960s. Additionally, several researchers (Batchelor et al. 1978; Okada et al. 1978; Perdikaris and Beim 1988; Perdikaris et al. 1994; Petrou et al. 1994; Sonoda and Horikawa 1982; Tanihira et al. 1988) have been working on the fatigue behavior of reinforced concrete bridge decks. There is, however, a paucity of research investigating the fatigue performance of reinforced concrete beams strengthened with FRP composite sheets and laminates.

Fatigue Behavior of Plain Concrete

The fatigue strength of a concrete member corresponding to a life of ten million cycles is assumed to be about 55% of the initial static strength of the member. Factors like the range of loading, rate of loading, eccentricity of loading, loading history, material properties, and environmental conditions influence fatigue strength (ACI Committee 215 1992). Hordijk and Reinhardt (1992) studied the fatigue behavior of plain concrete and concluded that the propagation of cracks leads to failure of concrete, although the exact mechanism is not clear.

Fatigue Behavior of Steel Reinforcement

Fatigue failure of reinforcing steel is caused by a microcrack that initiates at a stress concentration on the bar surface. The crack gradually propagates as the stress continues to cycle. Sudden fracture occurs when the crack reaches a critical length at which its propagation becomes unstable. Thus, the fatigue life of reinforcing steel equals the time or number of cycles to crack initiation plus the duration of crack growth. Crack initiation typically occurs at the location of the largest stress concentration, usually at the intersection of transverse lugs and longitudinal ribs.

The fatigue strength of reinforcing bars depends on chemical composition, microstructure, inclusions, minimum stress, bar size, type of beam, geometry of deformations, yield, and tensile strength, etc. (ACI Committee 215 1992). The lowest stress range known to have caused a fatigue failure of the bars in a concrete beam is 145 MPa (Helgason and Hanson 1974). Additionally, the fatigue strength of reinforcing bars may be only one-half of the fatigue strength of coupons machined from samples of the bars (Corley et al. 1978). Since fatigue

[1]Grad. Res. Asst., Dept. of Civ. and Envir. Engrg., Rutgers Univ., New Brunswick, NJ 08855; formerly, Grad. Res. Asst., Dept. of Civ. and Envir. Engrg., Univ. of South Carolina, Columbia, SC 29208.

[2]Assoc. Prof., Dept. of Civ. and Envir. Engrg., Univ. of South Carolina, Columbia, SC 29208.

[3]Asst. Prof., Dept. of Civ. and Envir. Engrg., Univ. of South Carolina, Columbia, SC 29208.

Note. Discussion open until April 1, 2002. To extend the closing date one month, a written request must be filed with the ASCE Manager of Journals. The manuscript for this paper was submitted for review and possible publication on June 2, 2000; revised December 27, 2000. This paper is part of the ***Journal of Composites for Construction***, Vol. 5, No. 4, November, 2001. ©ASCE, ISSN 1090-0268/01/0004-0246–0253/ $8.00 + $.50 per page. Paper No. 22178.

strength is significantly affected by physical characteristics (lug geometry, diameter of the bars, and the grade of the bar), the variables related to these physical characteristics are of great concern (Corley et al. 1978).

Helgason and Hanson (1974) conducted a statistical analysis of test data from deformed bars tested axially in air. They concluded that the lowest average stress range on reinforcing steel that causes fatigue failure is 165 MPa and derived the following fatigue life relationship:

$$\log(N) = 6.969 - 0.0055\sigma_r \quad (1)$$

where N = number of cycles to failure; and σ_r = stress range applied to the steel in MPa.

Another analysis of experimental results, conducted by Moss (1982), derived the following fatigue life relationship for axially loaded reinforcing bars embedded in concrete:

$$N\sigma_r^m = K \quad (2)$$

where σ_r^m = stress range within tensile reinforcing steel in MPa; N = number of cycles to failure; m = inverse slope of log σ_r–log N curve = 8.7; $K = 0.11 \times 10^{29}$ for the mean line of the relationship; and $K = 0.59 \times 10^{27}$ for the mean minus two standard deviations line.

As the concrete in a reinforced concrete beam cracks in the tension zone of the beam, high strain values and hence high stresses in the bar spanning the crack are developed. Since the maximum stress occurs at limited locations, it is less likely that these coincide with defects in the bar. This results in a longer fatigue life for reinforcing steel embedded in a concrete beam as compared with reinforcing steel subjected to the same stress range in air.

Fatigue Behavior of Reinforced Concrete

All the research cited above investigated the fatigue behavior of plain concrete and axially loaded reinforcing bars. However, the performance of a reinforced concrete beam also depends on the composite action between steel and concrete. Whereas an underreinforced member has its flexural fatigue performance dominated by the steel, a heavily reinforced member may fail in flexure or shear depending on whether the concrete or steel strength is critical. Research on reinforced concrete beams (Mallet 1991) concluded that shear fatigue failure could occur in beams with or without stirrups, the fatigue life of reinforcement being much the same whether it is longitudinal tensile reinforcement or transverse stirrups. As the fatigue loading of a beam progresses, and the subsequent cracks propagate, there is a redistribution of stress; thus, fatigue failure is not always by the same mechanism as static failure (Barnes and Mays 1999).

ACI Committee 215 (1992) recommends that the maximum allowable stress range in straight deformed reinforcement in reinforced concrete beams, σ_r, be given as

$$\sigma_r = 161 - 0.33\sigma_{\min} \quad (3)$$

where $\sigma_{\min}$ = minimum stress (tension positive, compression negative) in MPa; σ_r may not be taken as less than 138 MPa.

Fatigue Behavior of Reinforced Concrete beams Strengthened with FRP Composites

Composite materials generally exhibit much greater fatigue life than other structural materials. In materials with a crystalline structure, like steel, fatigue microcracks initiate at a defect and propagate, forming a crack that continues to grow with each load cycle. Conversely, the individual fibers within FRP composites have relatively few defects, and any crack that forms in the composite matrix does not propagate across the fiber. This contributes to the good fatigue performance of FRP composites. (Conolly 1992)

Meier et al. (1992) reported two fatigue tests of reinforced concrete beams strengthened with a glass/carbon-hybrid sheet. In the first test, the sheet was 0.3×200 mm in cross section and was bonded to the tensile surface of the beam. The beam had a span of 2,000 mm, was 300 mm wide, and 250 mm deep. Conventional reinforcement consisted of two 8 mm bars in the tension zone. The beam was tested in third point bending. The load was cycled from 1 to 19 kN at a frequency of 2 Hz; the corresponding maximum stress range in the rebar was 386 MPa. Failure of the beam occurred after 480,000 cycles.

The second test was conducted on a tee-beam having a 6,000 mm span strengthened with a carbon FRP (CFRP) sheet 1.0×200 mm in cross section. Tension zone reinforcement consisted of four 26 mm bars. The beam was cycled in third point bending from 126 to 283 kN (ultimate capacity of 815 kN), the corresponding stress range in the rebar was 131 MPa. After 10.7×10^6 cycles, the test temperature was increased to 40°C and the relative humidity to 95%. The first reinforcing bar failed at 12×10^6 cycles, with failure of the beam occurring at 14×10^6 cycles.

Barnes and Mays (1999) reported on fatigue tests of two reinforced concrete beams and three reinforced concrete beams strengthened with CFRP plates. All five beams were 2,300 mm long, 130 mm wide, and 230 mm deep and tested in third point bending. The steel reinforcement consisted of three 8 mm rebars in the tension zone. The maximum load range varied from 26 to 39% of the ultimate load. The stress range in the reinforcing steel was kept the same for both the plated and nonplated beams.

Results from these tests indicated that the beams failed in a primary flexural mode. Initial failure was due to the steel fracture rather than failure of the concrete, adhesive, or fracture of the FRP plates. There were no distinguishable differences in behavior between the strengthened and nonstrengthened beams during load cycling. The number of cycles to failure varied according to the applied load range.

Shahawy and Beitelman (1999) tested six tee-beams under fatigue loading. The load range was 0–25% of the ultimate load. Two beams were used as control beams, two were fully wrapped with two layers of CFRP, and two were wrapped with three layers of CFRP. One of the two control beams was fully wrapped with two layers of CFRP after 150,000 cycles, after it was severely cracked. In that case, the number of loading cycles to failure was increased to 2×10^6 compared with the nonstrengthened beam, which failed at 295,000 cycles. The two specimens with two layers of FRP exhibited fatigue lives of approximately 1.8×10^6 cycles and the two with three layers reached 3×10^6 cycles.

It is noted that the stirrups in all specimens were tack-welded to the main reinforcing bars, which is known to negatively impact the fatigue life of the reinforcement. The results of these tests indicated that the failure was based on the fracture of steel. It was concluded that the use of FRP increases the fatigue life of the beams as well as that the increase of the number of layers of CFRP results in a further increase of the fatigue life of the beams.

EXPERIMENTAL PROGRAM

Experiments conducted for this project involve seventeen reinforced concrete beams. Nine were strengthened with a commercially available GFRP composite system. All beams were tested in third-point bending. Three beams were initially tested under static load in order to establish their ultimate load-carrying capacity.

All beams were fabricated at the same time using the same

reinforcing steel and concrete. This was done in order to decrease the variability associated with the materials. Concrete was provided by a local ready-mix concrete company. After the concrete was placed, the specimens were moist cured for seven days. The beams were cast more than six months before the initiation of the experiments. The uniaxial compressive strength of the concrete mixture was evaluated using standard 150 × 300 mm cylinders. The average compressive strength at the time of testing was 39.3 MPa.

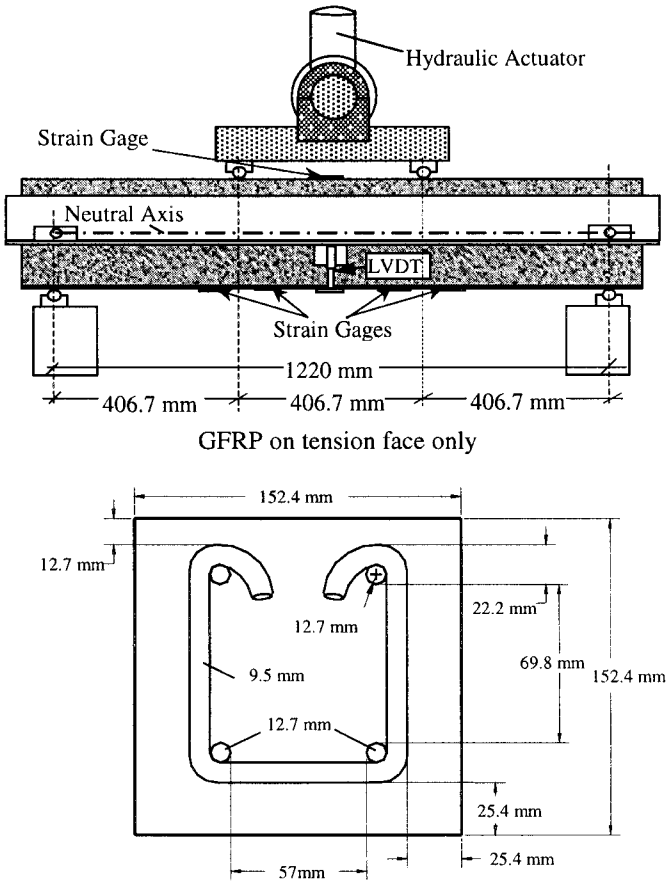

FIG. 1. Test Setup and Specimen Details

The reinforced concrete beams prepared for this project were 1,321 mm long, having a cross section of 152 × 152 mm and were simply supported over a 1,220 mm span. The design of shear and flexural reinforcement was based on ACI 318 Code (ACI 1999) procedures. Two 12.7 mm bars were selected as flexural reinforcement, and two more were placed in the compression region for fabrication ease. Twenty 9.5 mm stirrups were placed in the beam as shear reinforcement at a spacing of 50 mm in the two outer thirds of the beam, and two stirrups were spaced evenly in the center, zero-shear/constant-moment third of the beam. The design of the flexural and shear steel reinforcement ensured a flexural failure of the beams. A clear cover of 25 mm was provided on all sides except the top surface, which was provided with 13 mm. The yield strength of the steel was 427 MPa and its elongation at yield was 2,350 microstrain. Specimen details are shown in Fig. 1.

A commercially available unidirectional GFRP system was used in this study. The system included a primer, epoxy resin system, and glass fiber fabric was installed according to the manufacturer's recommended procedure. The glass fibers have a reported strength of 1,730 MPa and a stiffness of 72,400 MPa. The GFRP composite system has a coupon tensile strength of approximately 330 N/(mm·ply) and a stiffness of approximately 14 kN/(mm·ply) (Pessiki et al. 2001). Strength and modulus of the FRP are given in units of force per unit dimension perpendicular to the principle direction of the fibers per ply [such as N/(mm·ply)]. Such units are independent of thickness of the FRP. This is particularly useful where hand layed-up material is used since, in this case, thickness depends on parameters such as fiber volume ratio, fabric geometry, and lay-up technique (Pessiki et al. 2001). Strengthened specimens were allowed to cure at least 10 days after the FRP application.

The specimens are labeled as follows: ''N'' indicates nonstrengthened reinforced concrete beams, and ''S'' indicates beams strengthened with GFRP composite sheets. Each beam was numbered in consecutive order. All the strengthened

TABLE 1. Summary of Monotonic and Fatigue Test Results

Beam	Testing frequency	Ultimate applied load, P_{ult} (kN)	Applied load at yield, P_y (kN)	Applied Load (kN) max	Applied Load (kN) min	P_{max}/P_{ult}	P_{max}/P_y	Strain on Steel (microstrain) max	Strain on Steel (microstrain) min	Number of cycles to failure, N	δ (mm)	δ/δ_{ult}
(a) Nonstrengthened reinforced concrete beams												
N-1	monotonic	73.8	58.2	NA	NA	NA	NA	2,400[a]	NA	NA	15.5	NA
N-2	monotonic	73.3	58.2	NA	NA	NA	NA	2,460[a]	NA	NA	15.5	NA
N-4	3 Hz	—[b]	—[b]	31.2	3.3	0.42	0.53	950	60	2,000,000	17.7	1.14
N-5	3 Hz	—[b]	—[b]	35.6	3.3	0.48	0.61	1,100	60	2,000,000	16.7	1.08
N-8	3 Hz	—[b]	—[b]	40.0	3.3	0.52	0.68	1,493	124	650,000	—	—
N-3	2 Hz	—[b]	—[b]	43.6	3.3	0.59	0.74	1,701	85	275,000	15.2	0.98
N-6	2 Hz	—[b]	—[b]	53.4	4.4	0.73	0.91	2,010	143	155,000	14.3	0.92
N-7	2 Hz	—[b]	—[b]	62.3	3.3	0.85	1.05	2,350	99	80,000	17.9	1.16
(b) Reinforced concrete beams strengthened with one ply of GFRP												
S-4	monotonic	109.7	80.1	NA	NA	NA	NA	2,500[a]	NA	NA	14.2	NA
S-11	3 Hz	—[c]	—[c]	40.0	3.3	0.36	0.50	1,274	105	6,000,000	14.9	1.05
S-10	3 Hz	—[c]	—[c]	44.5	3.3	0.41	0.55	1,419	106	685,000	16.0	1.13
S-2	3 Hz	—[c]	—[c]	46.7	2.2	0.43	0.58	1,410	66	880,000	—	—
S-5	3 Hz	—[c]	—[c]	48.9	4.0	0.45	0.61	1,477	101	800,000	14.3	1.01
S-7	3 Hz	—[c]	—[c]	53.4	3.3	0.49	0.67	1,580	99	570,000	15.8	1.11
S-9	2 Hz	—[c]	—[c]	57.8	3.3	0.53	0.72	1,825	110	235,000	13.2	0.93
S-6	2 Hz	—[c]	—[c]	64.5	4.4	0.59	0.81	2,080	160	126,000	13.8	0.97
S-8	2 Hz	—[c]	—[c]	80.1	4.0	0.73	1.0	2,350	135	30,500	14.2	1.00

[a]Strain in Reinforcing Steel at General Yield, P_y.
[b]Assumed to be same as N-1 and N-2.
[c]Assumed to be same as S-4.

beams were reinforced over their entire tensile surface with one ply of GFRP sheet (Fig. 1). Table 1 gives a summary of the beams and the different loading conditions. The maximum and minimum loads applied are presented for the fatigue tests. It should be noted that the maximum loads were determined based on the same percentages of yield strain in the steel reinforcement for both strengthened and nonstrengthened specimens. The required steel strains were subsequently determined based on a percentage of ultimate capacity of the beams determined from the static tests. The minimum applied load is necessary to avoid impact loads during cycling.

The tests were carried out using a 270 kN capacity hydraulic actuator. The actuator was operated under load control for the fatigue loading and under displacement control for the static tests. The load was applied at the third points of the beam within the 1,220 mm supported span. All contact points along the beam were supported with rollers to ensure that the load was applied evenly during testing (Fig. 1).

Strains on steel, concrete, and the GFRP sheet, as well as deflections at midspan, were recorded during testing in order to study their change under static and fatigue loading conditions. Two electrical resistance strain gauges were attached on opposite sides at the midspan of each longitudinal reinforcing bar to resolve the axial strain in the bar. Strain gauges were also located on the top concrete surface as well as on the GFRP sheet at selected locations (Fig. 1). The deflection at midspan was measured using a ''yoke'' deflection measuring system. This system, illustrated in Fig. 1, consists of an aluminum frame, bolted on at the neutral axis of the beam at the end supports and two LVDTs mounted on the ''yoke'' at midspan, one on each side of the beam. The LVDTs measure the deflection of the specimen through contact with two aluminum plates, bonded to the beam with epoxy. The average of the two measurements was taken as the net midspan deflection.

EXPERIMENTAL RESULTS

Experimental Results from Static Tests

Two nonstrengthened (N-1 and N-2) and one strengthened (S-4) beam were tested under monotonic loading conditions. The experimental results as well as the results of a theoretical plane sections model developed by Papakonstantinou (2000) are shown in Fig. 2. Yield load is defined as the load corresponding to a significant change in the slope of the total-deflection curve.

The strengthened beam is stiffer than the nonstrengthened beams before and after yielding of the reinforcing steel. It can be seen that the use of the GFRP composite sheet increases the ultimate load capacity of the beams by about 50%. On the other hand, there is less than a 10% reduction of ultimate deflection. The use of the GFRP system can strengthen the reinforced concrete beams without causing significant reduction of the ductility. The primary failure mechanism of the strengthened beam was yielding of the reinforcement and delamination of the GFRP sheet, while for the nonstrengthened beams, the primary failure mechanism was yielding of reinforcement.

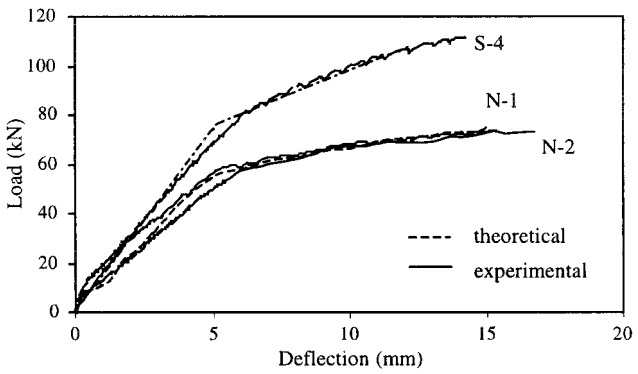

FIG. 2. Load versus Deflection Diagram for All Static Tests Including Theoretical Predictions

Experimental Results from Fatigue Tests

Fourteen beams were tested under cycling load at different load ranges. Six were nonstrengthened and eight were strengthened. The maximum load in each case was chosen based on a percentage of the maximum stress in the steel reinforcement as determined from the static tests and verified by strain measurements. The minimum load depended on the frequency of the loading and was selected to ensure stability of the test setup. For practical purposes, the maximum number of cycles applied to a single specimen was 2×10^6 cycles, except the last experiment (S-11), which was terminated after 7×10^6 cycles. During all fatigue tests, static tests were conducted on a regular basis in order to monitor the damage accumulation and its effect on the deflection and strain values.

The data in Table 1 includes the maximum and minimum applied loads and strain on the reinforcing bars, the ratio of applied load to the ultimate load observed in the static tests (P_{max}/P_{ult}), the ratio of the applied load to the yield load observed in static tests (P_{max}/P_y), the number of cycles to failure, and the ratio of the final deflections observed in the fatigue tests to the ultimate deflections observed in the static tests (δ/δ_{ult}). Data was not recorded for the last cycles for beams N-8 and S-2, since, in the first case, the beam failed suddenly and in the second the data acquisition system failed during the test.

Failure Mechanisms

All of the beams exhibited a similar primary mode of failure. In all cases, the failure was due to fatigue of the steel reinforcement as indicated by strain measurements. Yielding of the reinforcing steel is evident by the strain measurements, but is also indicated by the deflections and S-N curves, as discussed below. Flexural cracks were initiated after the first cycle and propagated as the number of applied cycles increased.

Debonding of GFRP sheet was a secondary failure mechanism for the strengthened beams. After the fatigue of steel reinforcement, the bonded GFRP sheet delaminated along the interface between the concrete and GFRP sheet or through the concrete immediately below the GFRP sheet. The delamination always started between two close flexural cracks. The first crack was initiated during the first cycles and the second one was usually formed 10,000–100,000 cycles before failure. Since fatigue of the steel reinforcement was the major factor contributing to the failure in the strengthened beams, the sec-

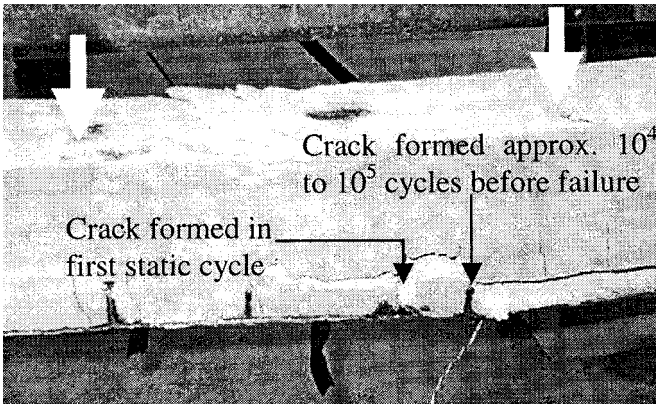

FIG. 3. Typical Failure of S Specimens (S-6)

ond crack seems to have started after the damage in the steel reinforcing bars was excessive. In many cases, the suddenly debonded GFRP sheet tore out the concrete cover already split vertically along the longitudinal reinforcing bars below the loading point. A typical failure of a strengthened beam is shown in Fig. 3. An exception to this behavior was specimen S-8, which was subjected to a maximum load equal to the yielding load (P_{max}/P_y = 1.0). Again, the primary failure mechanism was the fatigue of the reinforcement; however, the secondary mode of failure was the propagation of a major diagonal (shear) crack from a load point to its nearest support. Debonding of the GFRP sheet occurred at the base of this crack due to the relative displacement of the concrete blocks.

Both strengthened and nonstrengthened beams exhibited the same primary mode of failure, yielding of the steel reinforcement due to fatigue. The only noticeable difference between them is that shear cracks were also noticed in all the strengthened beams, usually very close to failure. In beams S-2, S-5, and S-7 shear cracks were initiated approximately 100,000 cycles before failure.

Deflection Measurements

The changes of the midspan deflections with the increase of the number of cycles for all beams tested under fatigue loading are given in Fig. 4. For each beam, the deflection was recorded during periodic monotonic loading tests. It can be seen that in all beams there was an initial increase of the midspan deflection, followed by a stable region where the deflection remained relatively constant through many cycles, followed by an abrupt increase of deflection just before failure. It can also be observed that, in all beams that failed after 400,000 cycles, there is a more gradual increase in the deflections as the beam approaches its fatigue life. This may be caused by a greater number of cracks resulting from increased cycling. Generally, however, the deflection remained the same until approximately 100,000 cycles before failure occurred, making the detection of an insipient failure very difficult.

The only beam that behaved differently was S-8, where the applied load was equal to the load necessary to cause yielding of the steel reinforcement (i.e., P_{max}/P_y = 1.0). The midspan deflection of S-8 increased continuously with respect to the number of cycles until failure.

It can also be seen that the final deflections of beams subjected to fatigue loading are very close to the average maximum deflections recorded during static tests. In Table 1, as well as in Fig. 4, it can be seen that the ratio of the maximum fatigue deflections to the ultimate static deflections (δ/δ_{ult}) was always close to 1. Therefore, it may be concluded that the load-deflection behavior of the strengthened and nonstrengthened beams subjected to cycling load is similar to their behavior under monotonic loading conditions.

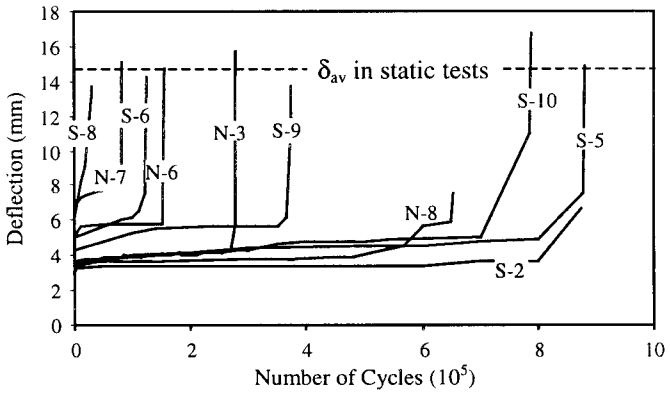

FIG. 4. Deflection versus Number of Cycles Due to Fatigue

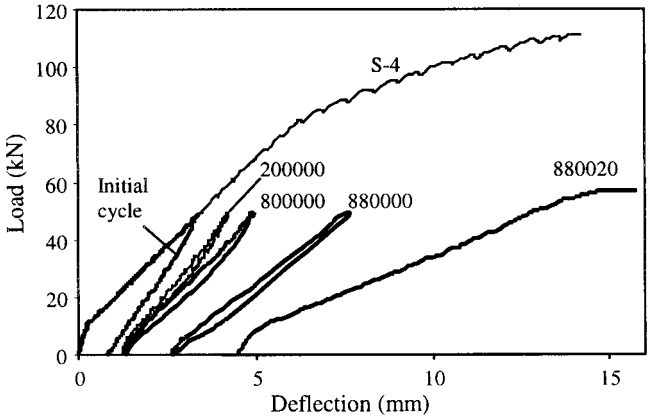

FIG. 5. Load versus Deflection Curves of S-5

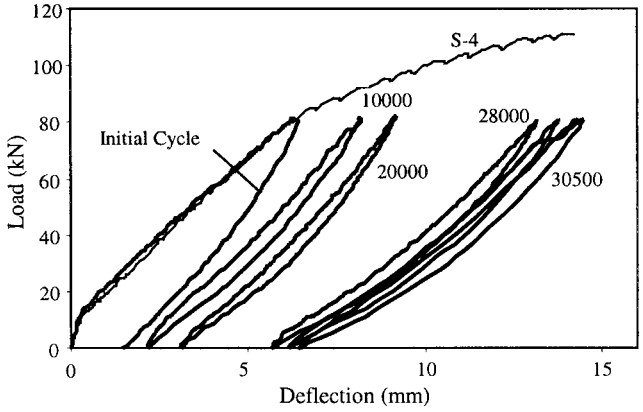

FIG. 6. Load versus Deflection Curves of S-8

Figs. 5 and 6 show a series of static load-deflection curves, conducted at different stages during the fatigue load history, for specimens S-5 and S-8, respectively. The load-deflection diagram of specimen S-4, tested under monotonic load, is also plotted. The deflection curves for beam S-8 indicate that the beam maintained most of its initial stiffness until close to failure. On the other hand, beam S-5 became notably more flexible at about 80,000 cycles before failure. Such a change, which occurred in all beams that failed after 400,000 cycles, may be attributed to the large number of small flexural cracks that were initiated and propagated slowly until failure. Conversely, in all the beams that failed before 400,000 cycles, a single flexural crack (except S-8, where it was a shear crack) led to failure.

Beam S-5 (Fig. 5), which failed at 880,020 cycles, became more flexible at 800,000 cycles, although it did not exhibit significant signs of damage until 20 cycles before failure. At 880,000 cycles the beam lost a large proportion of its stiffness and the maximum deflection increased by 35%. After 20 more cycles the beam failed.

Strain Measurements

The recorded strains on the steel reinforcement, GFRP sheet, and concrete (top surface) for S-7 and S-6 are presented in Figs. 7 and 8 respectively. Concrete compressive strains are shown as positive for ease of presentation. In both beams the strain in the reinforcing steel increased suddenly before failure, indicating yielding of the reinforcement. At that point, strains in the concrete and GFRP sheet increased but remained lower

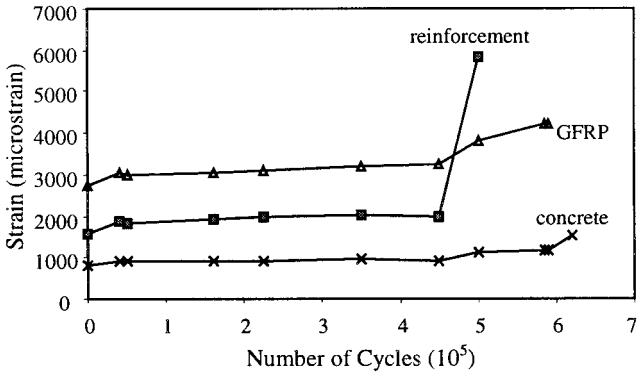

FIG. 7. Strain versus Number of Cycles for S-7

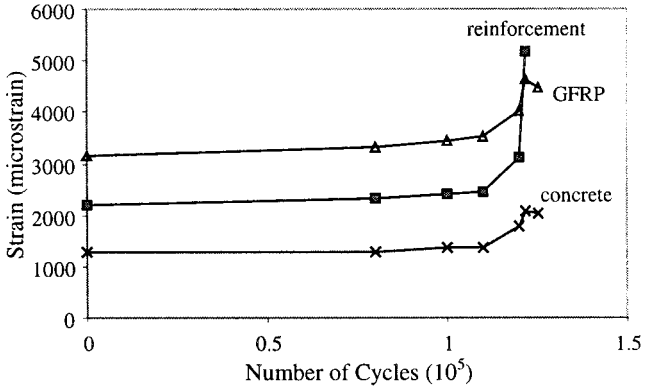

FIG. 8. Strain versus Number of Cycles for S-6

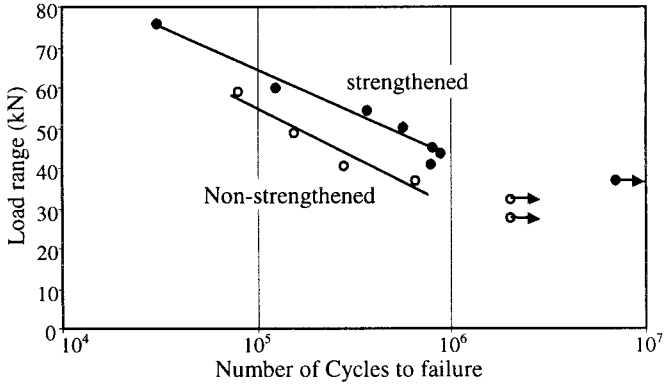

FIG. 9. Load Range versus Number of Cycles S-N Curves from Experimental Data

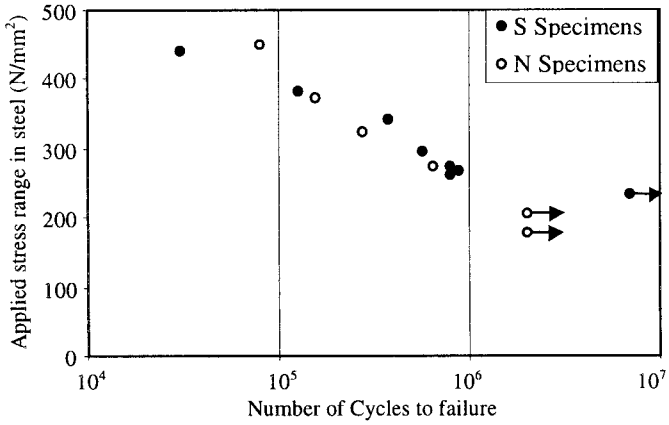

FIG. 10. Stress Range in Reinforcing Steel versus Number of Cycles S-N Curves from Experimental Data

than strains corresponding to expected ultimate behavior, 0.003 for concrete and 0.005 for the GFRP composite sheet. These figures indicate that the failure was due to the yielding of the reinforcing steel caused by fatigue. There was no distinguishable difference in behavior between the strengthened and nonstrengthened beams.

S-N Curves

The applied load range versus number of cycles to failure is presented in Fig. 9. Fitting curves from regression analysis of experimental results are also plotted. The regression analyses show that the fatigue life of the strengthened beams for the same load range is about three times greater than the fatigue life of the nonstrengthened beams. This is expected, since failure of all of the beams was based on the fatigue of steel reinforcement. GFRP composite sheet increases the strength and the stiffness of reinforced concrete beams (Fig. 2) and consequently reduces the stress on the steel reinforcement, prolonging the fatigue life of the beams.

The fact that the stress in the steel plays the most important role in fatigue performance of strengthened and nonstrengthened beams is verified by the S-N curve shown in Fig. 10, which presents the stress on the reinforcing steel for each of the beams. It is recalled that applied load levels were selected such that steel stresses were similar for strengthened and nonstrengthened specimens. This figure illustrates that strengthened and nonstrengthened beams subjected to the same stress in their reinforcing steel exhibit a similar number of cycles to failure.

The S-N curve presented in Fig. 11 includes the experimental data from the current study as well as that from other experiments of reinforcing steel tested axially in air and in concrete and for reinforced concrete beams strengthened with CFRP sheets. Although the graph includes experimental data from strengthened and nonstrengthened beams, there is a relatively small variation of the experimental data.

A regression curve based on the results of the present study is also shown in Fig. 11. The curve is given by the following equation (correlation coefficient, $R^2 = 0.9316$):

$$\log(N) = 6.677 - 0.00613 \cdot \sigma_r \quad (4)$$

where N = number of cycles to failure; and σ_r = stress range applied on the steel in MPa.

The fatigue life of strengthened and nonstrengthened reinforced concrete beams is about 40–300% higher than the fatigue life of reinforcing bars tested in air (Helgason and Hanson 1974). The fatigue life of reinforcement in air is used in the design of reinforced concrete for fatigue (Corly et al. 1978; ACI Committee 215 1992).

CONCLUSIONS

Conclusions are based on an experimental study conducted on seventeen 152 × 152 × 1,321 mm reinforced concrete beams. Three beams were initially tested under static load in order to establish their ultimate load-carrying capacity. Eight were strengthened with a commercially available GFRP strengthening system and tested under fatigue loading conditions. Six other nonstrengthened beams were also subjected to fatigue loading conditions. The following conclusions are drawn from this study:

1. The beams failed primarily due to fatigue of the steel reinforcement. Debonding of the GFRP composite sheet was a secondary mechanism in the strengthened beams.

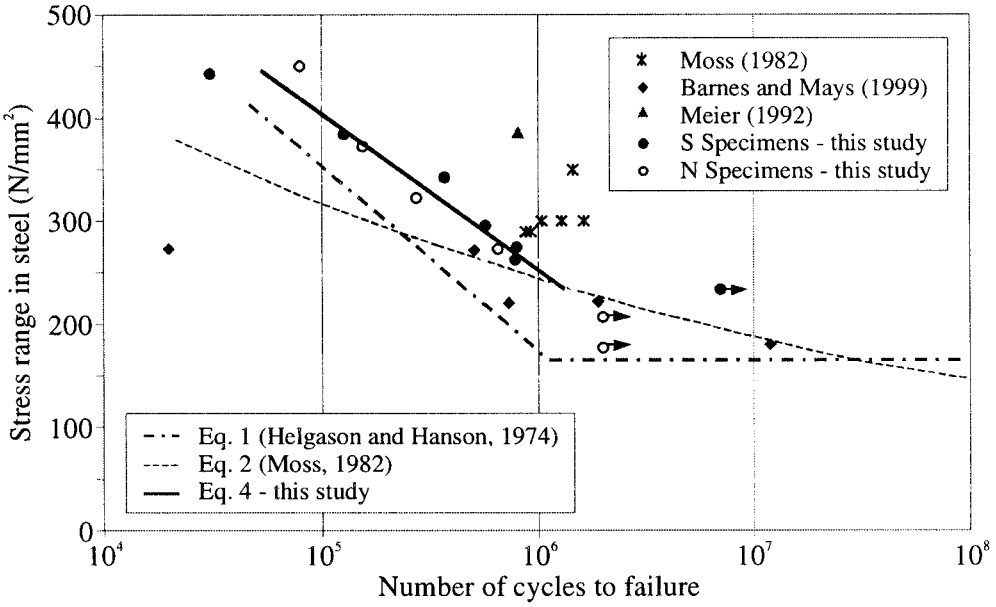

FIG. 11. Theoretical S-N Curves and Experimental Data from Various Researchers and Present Study

The failure was sudden. Signs of severe damage appeared only a few cycles before failure.

2. Since the fatigue failure mechanism does not indicate a failure of the FRP, the role of the GFRP composite sheet is to increase the strength and stiffness of the beam and thus to reduce the stress in the steel. Therefore, the fatigue life of strengthened beams is increased as compared with the nonstrengthened beams for the same applied load.
3. For the same applied stress range in the reinforcing steel, the fatigue life for the strengthened and nonstrengthened beams is the same. Therefore, existing fatigue models for reinforcing steel may be used to determine remaining life in GFRP strengthened reinforced concrete beams.
4. The ultimate deflection under fatigue loading conditions is the same as the ultimate deflection under static loading conditions. This indicates that the failure mechanism is the same under static and fatigue loading conditions.
5. The results of this study indicate that the maximum allowable stress range for reinforcing steel subject to fatigue loading of 161 MPa, recommended by ACI Committee 215 (1992), is appropriate and suitably conservative for reinforced concrete beams strengthened with FRP on their tension surfaces.

ACKNOWLEDGMENTS

The writers would like to acknowledge the financial support of South Carolina Universities Research and Education Foundation (SCUREF), Westinghouse Savannah River Company (WSRC), and the Department of Energy (DOE). Their support is greatly appreciated. Thanks are also due to Jennifer Gay, Baolin Wan, Stanley Young, and Ed Owens for their assistance in the laboratory. The opinions, findings, and conclusions expressed in this paper are those of the writers and not necessarily those of the SCUREF, WSRC, or DOE.

REFERENCES

ACI Committee 215 (1974). ''Consideration for design of concrete structures subjected to fatigue loading.'' *ACI J.*, 71(3), 97–121.
Balazs. G. L. (1991). ''Fatigue of bond.'' *ACI Mat. J.*, 88(6), 620–630.
Barnes, R. A., and Mays, G. C. (1999). ''Fatigue performance of concrete beams strengthened with CFRP plates.'' *J. Compos. for Constr.*, ASCE, 3(2), 63–72.
Batchelor, B., Hewitt, B. E., and Csagoly, P. (1978). ''An investigation of the fatigue strength of deck slabs of composite steel/concrete bridges.'' *Transp. Res. Rec., 664*, Transportation Research Board, Washington, D.C., 153–161.
Conolly, M. P. (1992). ''A substructing approach to the fatigue modeling of polymeric matrix composite materials.'' *Cyclic deformation, fracture, and nondestructive evaluation of advanced materials*, Vol, 2, ASTM, West Conshohocken, Pa., 265–277.
Corley, W. G., Hanson, J. M., and Helgason, T. (1978). ''Design of reinforced concrete for fatigue.'' *Res. and Devel. Bulletin RD059.01D*, PCA.
Halgason, T., and Hanson, J. M. (1974). ''Investigation of design factors affecting fatigue strength of reinforcing bars-statistical analysis.'' *Proc., Abeles Symp. on Fatigue of Concrete*, American Concrete Institute, Detroit, 107–138.
Hordijk, D. A., and Reinhardt, H. W. (1992). ''Numerical and experimental investigation into the fatigue behavior of plain concrete.'' *Proc., SEM VII Int. Congr. on Experimental Mech.*, Las Vegas NV.
Mallet, O. (1991). *Fatigue of reinforced concrete*, HMSO, London.
Mays, G. C., and Tilly, G. P. (1982). ''Long endurance fatigue performance of bonded structural joints.'' *Int. J. Adhesion and Adhesives*, Guifford, U.K., 2(2), 109–114.
Meier, U., Deuring, M., Meier, H., and Schwegler, G. (1992). ''Strengthening of structures with CFRP laminates: Research and applications in Switzerland.'' *Advanced Compos. Mat. in Bridges and Struct.*, K. W. Neale and P. Labossiere, eds. Canadian Society for Civil Engineers, Montreal.
Moss, D. S. (1982). ''Bending fatigue of high-yield reinforcing bars in concrete.'' *TRRL Supplementary Rep. 748*, Transport and Road Research Laboratory, Crowthome, U.K.
Okada, K., Okamura, H., and Sonoda, K. (1978). ''Fatigue failure mechanism of reinforced concrete bridge deck slabs.'' *Transp. Res. Rec. No. 664*, Transportation Research Board, Washington, D.C., 136–144.
Papakonstantinou, C. G. (2000). ''Fatigue performance of reinforced concrete beams strengthened with glass fiber reinforced polymer composite sheets.'' MS thesis, University of South Carolina, Columbia, S.C.
Perdikaris, P. C., and Beim, S. (1988). ''RC bridge decks under pulsating and moving load.'' *J. Struct. Engrg.*, ASCE, 114(3), 591–607.
Perdikaris, P. C., Petrou, M. F., and Wang, A. (1994). ''Fatigue strength and stiffness of concrete bridge decks.'' *Final Rep. FHWA-OH-93-016*, Case Western Reserve University, Cleveland, Ohio.
Pessiki, S., Harries, K. A., Kestner, J., Sause, R., and Ricles, J. M. (2001). ''Axial behavior of concrete confined with fiber reinforced composite jackets.'' *J. Compos. in Constr.*, ASCE, 5(4), 237–245.
Petrou, M. F., Perdikaris, P. C., and Wang, A. (1994). ''Fatigue behavior of non-composite concrete bridge deck models.''*Transp. Res. Rec. No. 1460*, Transportation Research Board, Washington, D.C., 73–80.
Pochanart, S., and Harmon, T. (1989). ''Bond-slip model for generalized excitations including fatigue.'' *ACI Mat. J.*, 86(5), 465–469.
Rehm, G., and Eligehausen, R. (1979). ''Bond of ribbed bars under high cycle repeated loads.'' *ACI J.*, 76(1), 297–313.
Shah, S. P., and Chandra, S. (1970). ''Fracture of concrete subjected to cyclic and sustained loading.'' *ACI J.*, 67(10), 816–824.

Shahawy, M., and Beitelman, T. E. (1999). ''Static and fatigue performance of RC beams strengthened with CFRP laminates.'' *J. Struct. Engrg.*, ASCE, 125(6), 613–621.
Sonoda, K., and Horikawa, T. (1982). ''Fatigue strength of reinforced concrete slabs under moving loads.'' *Proc., IABSE Colloquium, Fatigue of Steel and Concrete Struct.*, International Association for Bridge and Structural Engineering, Zurich.
Tanihira, T., Sonoda, K., Horikawa, T., and Kitoh, H. (1988). ''Low cycle fatigue characteristics of bridge deck RC slabs under the repetition of wheel loads.'' *Proc., Pacific Concrete Conf.*, New Zealand, 381–392.
Tilly, G. P. (1979). *Fatigue of steel reinforcement bars in concrete: a review. Fatigue of engineering materials and structures*, Pergamon, London, 251–268.
Tilly, G. P., and Moss, D. S. (1982). ''Long endurance fatigue of steel reinforcement.'' *Proc., ABSE Coll.*, Lausanne, Switzerland.
Verna, J. R., and Stelson, T. E. (1962). ''Failure of small reinforced concrete beams under repeated loads.'' *ACI J.*, 59(9), 1489.

NOTATION

The following symbols are used in this paper:

K = constant defined by Moss (1982);
m = inverse slope of log σ_r—log N curve;
N = number of cycles to failure;
P_{max} = maximum load applied to beam;
P_{ult} = ultimate load capacity beam;
P_y = load at yielding of beam;
δ = maximum deflection after fatigue loading of beam;
δ_{av} = average ultimate static deflection of strengthened and non-strengthened beams;
δ_{ult} = ultimate static deflection of beam;
σ_{min} = minimum stress in tensile reinforcing steel; and
σ_r = stress range in tensile reinforcing steel.